Synthesis and thermomechanical behavior of (qua)ternary thiol-ene(/acrylate) copolymers

Scott E. Kasprzak [a,*], Blanton Martin [b], Tulika Raj [c], Ken Gall [a,d]

[a] G.W.W. School of Mechanical Engineering, Georgia Institute of Technology, Atlanta, GA 30332, USA
[b] Dept. of Chemistry & Biochemistry, Georgia Institute of Technology, Atlanta, GA 30332, USA
[c] W.H.C. Dept. of Biomedical Engineering, Georgia Institute of Technology, Atlanta, GA 30332, USA
[d] Materials Science & Engineering, Georgia Institute of Technology, Atlanta, GA 30332, USA

ARTICLE INFO

ABSTRACT

The objective of this work is to characterize and understand the structure-to-thermomechanical property relationship in thiol-ene and thiol-ene/acrylate copolymers in order to complement the existing studies on the kinetics of this polymerization reaction. Forty-one distinct three- and four-part mixtures were created with systematically varied functionality, chemical structure, type and concentration of crosslinker. The resulting polymers were subjected to dynamic mechanical analysis and tensile testing at their respective glass transition temperature, T_g, to quantify and understand their thermomechanical properties. The copolymer systems exhibited a broad range of T_g, rubbery modulus – E_r and failure strain. The addition of a difunctional high-T_g acrylate to several three-part systems increased the resultant T_g and E_r. Higher crosslink densities generally resulted in higher stress and lower strain at failure. The tunability of the thermomechanical properties of these copolymer systems is discussed in terms of inherent advantages and limitations in light of pure acrylate systems.

© 2009 Elsevier Ltd. All rights reserved.

1. Introduction

For the better part of a century, (meth)acrylates have formed a versatile class of polymers that play a major role in military and commercial products, from airplane canopies [1–4] and vehicle periscopes [5,6] to optical storage media [7,8], speakers [9], contact lenses [10], trophies [11], paints [12,13], coatings [14], and adhesives [15–18], as well as in industrial and academic research. Acrylates are popular because of their relatively low cost, ready availability, ease of monomer synthesis and polymer manufacture and processing, rapid polymerization kinetics, optical clarity, toughness, potential biocompatibility [19–22], and the broad range of achievable properties [23]. Photopolymerization of acrylates, in particular, is popular because of its relatively low energy requirements, capacity to be performed at ambient temperatures, and rapid speed [24–33]. Photolithography has featured acrylates, almost to the exclusion of other materials, since the very inception of the technique, due mostly to the acrylates' rapid curing kinetics and partly to the other aforementioned benefits. Typically, highly functional acrylate

monomers are used to insure rapid polymerization and pattern fidelity; these highly crosslinked networks shrink less than networks formed from monomers with lower functionality. As a direct result of the high crosslink density (or low molecular weight between crosslinks) and monomer chemistry, these networks exhibit glassy behavior at ambient temperatures - e.g. high stiffness and low ductility. Acrylates are also used for shape memory applications [34–36], because the glass transition temperature (T_g) and rubbery modulus (E_r) can be tailored independently to suit a particular application. There is another class of polymer, called thiol-ene, that is also readily photopolymerizable and may be well suited to shape memory applications, complementing, and perhaps partially replacing the use of pure (meth)acrylates while expanding the range of achievable properties.

The thiol-ene reaction was first suggested by Posner in 1905 [37], but academic interest in this potential polymerization reaction remained relatively small, especially as compared to (meth)acrylate polymerization, until the last two decades. Interest in the thiol-ene reaction mechanism increased as distinct advantages over acrylate polymerization were discovered. Various researchers have shown that, unlike acrylates, thiol-ene reactions do not exhibit oxygen inhibition [38–42] and show reduced shrinkage [43–46], while retaining high optical clarity. Moreover, the thiol-ene reaction is the

* Corresponding author. Tel.: +1 302 690 3248.
  E-mail address: scott.kasprzak@gmail.com (S.E. Kasprzak).

only known free-radical addition polymerization reaction in which various chemical groups (e.g phenolic rings, ethylene glycol groups, ester groups) can be incorporated into the main chain backbones.

The thiol-ene polymerization reaction, first proposed by Kharasch and coworkers in 1938 (steps 1–4) [47], is shown in Fig. 1, assuming the –ene cannot homopolymerize. Termination is generally thought to occur by radical recombination [48], as seen in steps 7–9.

Steps 5 and 6 indicate how inhibition by oxygen is circumvented in this reaction – the peroxy radical still shows significant affinity for hydrogen abstraction from the thiol group, propagating the radical and allowing the reaction to continue. Note that, unlike acrylate chain-growth polymerization, in order to form a polymer from the thiol-ene mechanism, the thiol and –ene must both be at least difunctional. Reaction of purely difunctional monomers results in a linear polymer system (i.e. a thermoplastic), while the inclusion of monomers with higher functionality results in cross-linked network polymers, or thermosets. Monofunctional monomers simply act as chain terminators. To achieve full monomer conversion, a stoichiometric ratio of thiol and –ene functional groups is necessary, as is typical for a step growth polymerization.

However, before thiol-ene polymers can be translated into any application, such as shape memory use or in photolithography, a more rigorous understanding of the system behavior in bulk form is necessary. The majority of the studies on thiol-ene and thiol-ene/acrylate systems have focused on the reaction kinetics [42,43,48–59], while few have studied the thermo-mechanical properties of the resultant material in great detail [39,59–62]. A rigorous process-to-thermomechanical property study of thiol-ene/acrylates was performed by the Hoyle group [49], who studied the effect of acrylate structure on the properties of various ternary copolymers composed of one trithiol, one tri-ene, and one of a selection of (meth)acrylates.

Only one thiol and one –ene was studied, with variations in the structure of the acrylate being the variable of interest.

The current study, on the other hand, keeps the structure of the acrylate constant (when present) in an effort to elucidate heretofore unstudied effects of monomer structure on these networks formed via mixed-mode polymerization. This study aims to more thoroughly define the thermomechanical properties of a (qua)ternary thiol-ene/acrylate system with systematically varied functionality, chemical structure, type and concentration of crosslinker. The acrylate in the current study is the same as one from the Hoyle study [49], and though the functionalities differ, the –ene and thiol studied by the Hoyle group are structurally similar to some in the current study. The Hoyle study had a very strong kinetic study portion, while the mechanical property determination solely consisted of typical dynamic mechanical analysis and of room temperature impact measurements. This study aims to determine the mechanical behavior of the systems at equivalent macromolecular states (i.e T_g), whereas the mechanical testing in the Hoyle study was solely performed at room temperature – irrespective of the polymers' T_g's - in an effort to identify a polymer system with optimal impact resistance under ambient conditions.

Since the thermomechanical properties of a material are a critical parameter in the design of a device, a goal of the current research is to photopolymerize a series of thiol-ene monomer mixtures with systematically varied crosslinker concentration to determine the effect of this parameter on the properties of the copolymer. Additionally, the effect of adding a high T_g diacrylate at selected concentrations to chosen thiol-ene base systems will be investigated to determine the effect that the acrylate has on the overall group conversion and resultant properties of the quaternary copolymer. In essence, the results of this study will complement the results of earlier polymerization kinetics studies by providing the
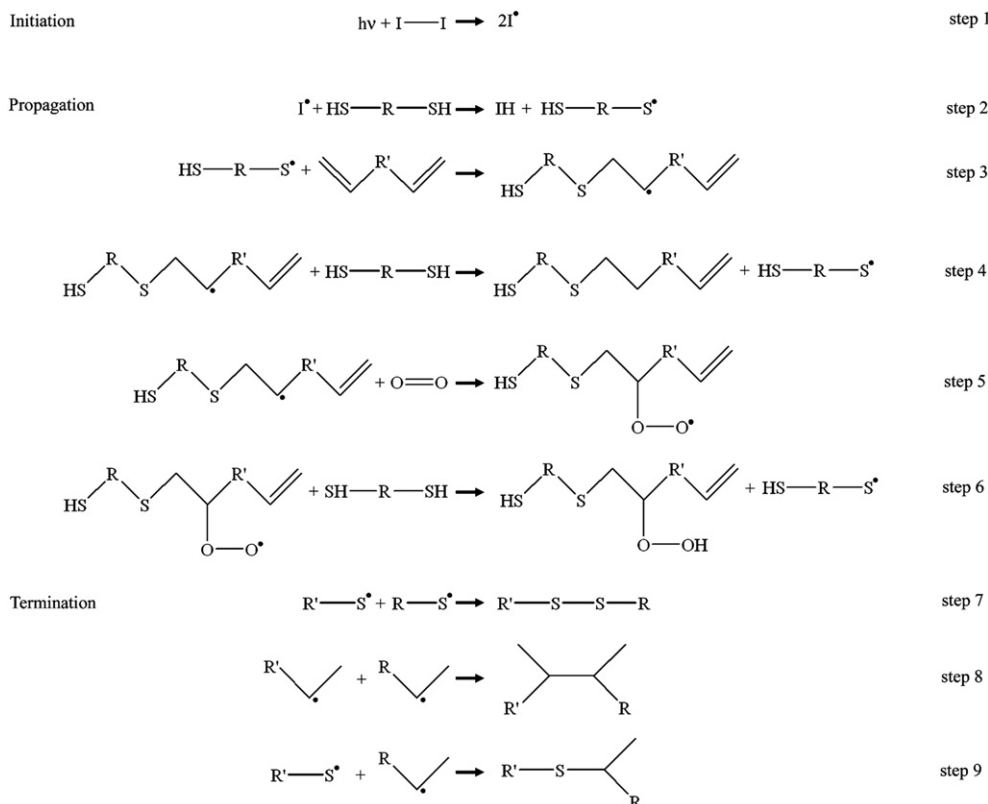

Fig. 1. Thiol-ene reaction schematic.

second half of the thiol-ene(/acrylate) polymerization process-property map.

2. Experimental

For clarity of presentation, the polymer composition labeling is centered around the equivalence of functional groups and is broken into two parts – the thiol functional group component, $t_f$mol%, and the –ene functional group component, $e_f$mol% – each totaling 100% and insuring a stoichiometric ratio of the functional groups. Acrylate functional groups, when added, are indicated by $a_f$mol%; terminology and labeling for compositions including acrylates differ slightly from the ternary mixtures and will be explained appropriately.

2.1. Materials

Forty-one monomer mixtures (shown in Table 1) were made of various combinations of three or four of the five monomers whose chemical structures and abbreviations are shown in Fig. 2, with the exception of one composition consisting entirely of Bisphenol A ethoxylate diacrylate, $M_n = 512$ [BPAEDA(512)]. 2,2-dimethoxy-2-phenylacetophenone (DMPA) was used as the UV photoinitiator. The naming convention used herein highlights a critical parameter of the

Table 1
Monomer mixtures used in study.

Mix	Mix Name/Chemical	$t_f$mol%		$e_f$mol%		$a_f$mol%
		PDT	PETMP	TMPDAE	TATATO	BPAEDA(512)
1	10PETMP (10P)	90	10	100	–	–
2	13.33PETMP	86.67	13.33	100	–	–
3	16.67PETMP	83.33	16.67	100	–	–
4	20PETMP	80	20	100	–	–
5	30PETMP	70	30	100	–	–
6	40PETMP	60	40	100	–	–
7	50PETMP (50P)	50	50	100	–	–
8	60PETMP	40	60	100	–	–
9	70PETMP	30	70	100	–	–
10	80PETMP	20	80	100	–	–
11	90PETMP (90P)	10	90	100	–	–
12	100PETMP	–	100	100	–	–
13	10P + 25BPAEDA(512)	90	10	100	–	+25
14	10P + 50BPAEDA(512)	90	10	100	–	+50
15	10P + 75BPAEDA(512)	90	10	100	–	+75
16	50P + 25BPAEDA(512)	50	50	100	–	+25
17	50P + 50BPAEDA(512)	50	50	100	–	+50
18	50P + 75BPAEDA(512)	50	50	100	–	+75
19	90P + 25BPAEDA(512)	10	90	100	–	+25
20	90P + 50BPAEDA(512)	10	90	100	–	+50
21	90P + 75BPAEDA(512)	10	90	100	–	+75
22	10TATATO (10T)	100	–	90	10	–
23	20TATATO	100	–	80	20	–
24	30TATATO	100	–	70	30	–
25	40TATATO	100	–	60	40	–
26	50TATATO (50T)	100	–	50	50	–
27	60TATATO	100	–	40	60	–
28	70TATATO	100	–	30	70	–
29	80TATATO	100	–	20	80	–
30	90TATATO (90T)	100	–	10	90	–
31	100TATATO	100	–	–	100	–
32	10T + 25BPAEDA(512)	100	–	90	10	+25
33	10T + 50BPAEDA(512)	100	–	90	10	+50
34	10T + 75BPAEDA(512)	100	–	90	10	+75
35	50T + 25BPAEDA(512)	100	–	50	50	+25
36	50T + 50BPAEDA(512)	100	–	50	50	+50
37	50T + 75BPAEDA(512)	100	–	50	50	+75
38	90T + 25BPAEDA(512)	100	–	10	90	+25
39	90T + 50BPAEDA(512)	100	–	10	90	+50
40	90T + 75BPAEDA(512)	100	–	10	90	+75
41	100BPAEDA(512)	–	–	–	–	100

study – the concentration of crosslinker. All ternary mixtures used DMPA as the photoinitiator at a concentration of one initiator molecule per 1000 –ene groups, or +0.1 $e_f$mol% (the plus is included to denote that it is additive, not substitutive for the –ene functionalities). DMPA acted as the photoinitiator in quaternary mixtures as well, but at a concentration of one initiator molecule per 1000 –ene and acrylate groups (+0.1 e_f+a_fmol%). The pure BPAEDA(512) reference sample contained DMPA at one part per 1000 acrylate groups (+0.1 $a_f$mol% or +0.1 wt%). All materials were obtained from Sigma Aldrich and were used as received.

2.2. Methods

Polymer sheets were created by injecting monomer solution into a mold consisting of two slides separated by 1 mm spacers and secured with binder clips, then exposing the mold to a UVP Blak-Ray® 365 nm UV light (intensity ∼8 mW/cm²) for 5 min. Prior to injection, the slides were thoroughly cleaned with acetone; for the 10PETMP mixture, RainX was applied to the slides to act as a release agent, due to the tacky nature of the finished polymer. A minimum of three sheets (or slides) of each mixture were polymerized.

Samples for dynamic mechanical analysis (DMA) were obtained by excising a portion of the polymer sheet with a razor blade and polishing the edges with 800- and then 1200-grit silicon–carbide sandpaper, to arrive at final specimen dimensions of approximately 20 mm × 4.5 mm × 1 mm. A TA Instruments Q800 DMA was used to obtain the storage modulus (E') and loss factor (tan δ) curves in tensile mode. The samples ($n \geq 2$) were cooled to $-100\,°C$, equilibrated for 2 min, and then ramped at a rate of 2 °C/min to 120 °C. The frequency was set to 1 Hz, the force track was set to 150%, and the strain level was set to 0.1%. T_g was determined by the peak of the tan(δ) curve [23,34–36,48,59,63], and E_r was defined as the lowest point in the storage modulus curve.
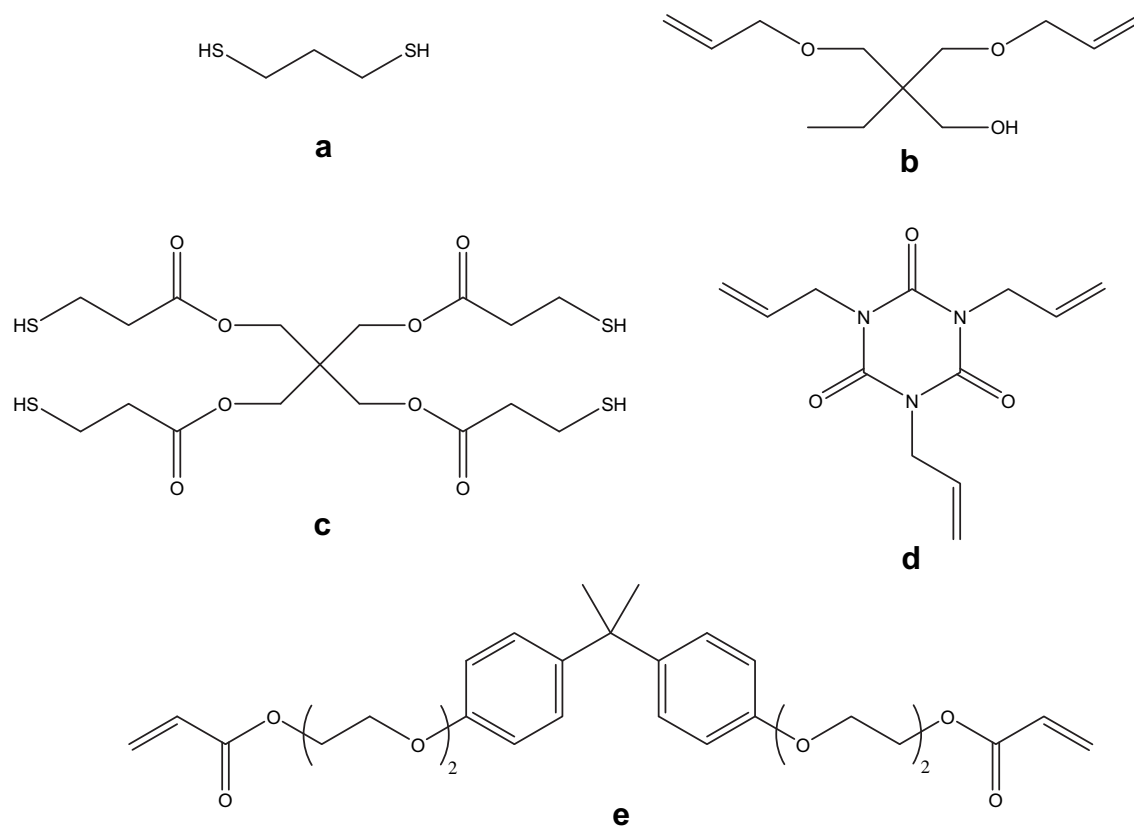
Samples for Fourier-transform infrared (FTIR) spectroscopy ($n \geq 2$) were scanned in monomer form, polymerized under the UV light for 5 min as per the aforementioned procedure, and then scanned again to determine overall group conversion. The solutions were injected between sapphire windows with a gap thickness of 2 μm and scanned at 16 scans per spectrum with a resolution of 4 cm^{-1} on a Varian FTS-7000 FTIR. Final group conversions were calculated using the ratio of the polymer to monomer absorbance peak area at each group's signature wavenumber [48]: 1640 cm^{-1} for the vinyl group, 2570 cm^{-1} for thiol, and 3085 cm^{-1} for the allyl ether C=C bond. Note that the contribution of the allyl ether to the –ene signal was accounted for by using the peak at 3085 cm^{-1}, thereby allowing separation of the –ene and acrylate group conversions.

Sol-fraction testing was performed by cutting 5 mm × 5 mm × 1 mm samples of six specific mixtures ($n = 3$) and taking the dry mass of each. The samples were subsequently soaked in 2 mL of acetone for 48 h to swell the networks and wash out excess monomer and other impurities. The samples were then dried in an oven at 60 °C for 72 h, and then allowed to acclimate to room conditions for an additional 72 h. The masses of the samples were then measured again, and the mass loss was calculated using the difference between the masses prior to and following the acetone soak and drying periods.

Tensile testing samples ($n \geq 3$) were excised from the polymer sheets by an ASTM D638 type V punch. The edges of the samples were polished with 800-grit silicon–carbide sandpaper to remove visible defects. The samples were strained at their respective T_g's at a rate of 1 mm/min (strain rate: ∼0.21 s^{-1}) until failure on an MTS Instruments Insight 2 mechanical load frame with a 100 N load cell. The experimental temperature was maintained by a Thermcraft, Inc. model LBO-14-8-5.25-1X-J8249_1A thermal chamber outfitted

Fig. 2. Chemical structures of studied monomers. (a) 1,3-propanedithiol (PDT), (b) trimethylolpropane diallyl ether (TMPDAE), (c) pentaerythritol tetrakis(3-mercaptopropionate) (PETMP), (d) 1,3,5-triallyl-1,3,5-triazine- 2,4,6(1H,3H,5H)-trione (TATATO), (e) Bisphenol A ethoxylate diacrylate, M_n 512 (BPAEDA(512)).

with liquid nitrogen cooling. The samples and equipment in the chamber were allowed to equilibrate for ten minutes at the testing temperature prior to test commencement. A laser extensometer was employed to measure the strain in the gage section of the sample, marked with adhesive-backed reflective tape. Sample experiments were run to ensure that the tape did not affect the samples' deformation behavior and mechanical response. However, for a full and accurate comparison among all samples, crosshead displacement is used for strain determination; laser extensometer data are unavailable for tests at subzero temperatures due to condensation on the reflective tape and thermal chamber window, which prevented proper and accurate readings.

3. Results

The first step in the characterization was dynamic mechanical anaylsis (DMA). Fig. 3 shows the progression of the storage modulus as the concentration of the PETMP crosslinker in a ternary mixture is increased from 10 $t_f$mol% to 100 $t_f$mol%. Fig. 4 shows the same progression graph for the ternary mixtures ranging from 10 $e_f$mol% TATATO to 100 $e_f$mol% TATATO. In both figures, notably, the rubbery modulus increases several orders of magnitude and the temperature for the onset of the glass transition shifts higher as more crosslinking agent is added.

Fig. 5 summarizes the T_g values for both types of ternary mixtures, as defined by the peak of the tan(δ) curve. For PETMP crosslinked mixtures, the T_g increases from −40.2 °C at the lowest concentration of PETMP to −16.0 °C at 100 $t_f$mol% PETMP. The T_g increases from −39.3 °C at the lowest concentration of TATATO to 35.3 °C at 100 $e_f$mol% TATATO. Fig. 6 summarizes the rubbery modulus values extracted from Figs. 3 and 4 for both types of

ternary mixtures. The rubbery modulus increases from 54.2 kPa at the lowest PETMP concentration to 8.65 MPa at 100 $t_f$mol% PETMP, and from 1.62 MPa at the lowest TATATO concentration to 14.6 MPa at 100 $e_f$mol% TATATO.

From these results, six mixtures were chosen for determination of the effect of acrylate addition – one low (10 $_f$mol%), one medium (50 $_f$mol%), and one high (90 $_f$mol%) amount of crosslinking for both -ene and thiol crosslinkers. 100 $_f$mol% crosslinker mixtures were excluded to help maintain somewhat similar chemistries in the
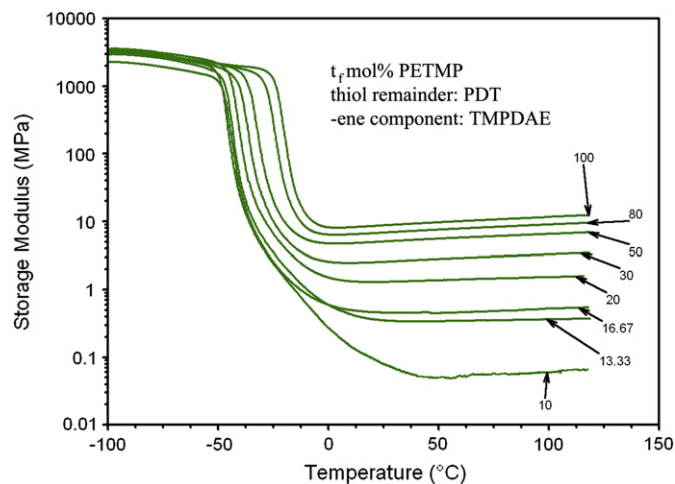
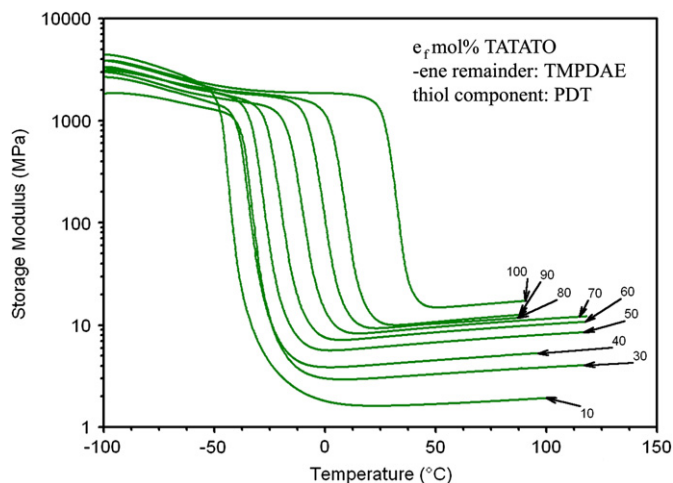**Fig. 3.** Progression of storage modulus for thiol-crosslinked ternary mixtures, by $t_f$mol% crosslinker.

Fig. 4. Progression of storage modulus for –ene-crosslinked ternary mixtures, by $e_f$mol% crosslinker.

Fig. 6. Rubbery moduli for various ternary mixtures of TMPDAE and PDT with either PETMP or TATATO.

base systems, i.e. all ternary systems, instead of a mixture of ternary and binary copolymers. The T_g values for the six selected base systems along with the three added concentrations (+25, +50, and +75 $_f$mol%) of BPAEDA(512) and pure BPAEDA(512) are shown in Fig. 7 and the rubbery moduli are shown in Fig. 8. Both the T_g and the E_r demonstrate a monotonic increase as BPAEDA(512) is added for all of the studied mixtures.

The copolymers were characterized with FTIR spectroscopy to determine final conversion of the functional groups in the monomer mixtures. Fig. 9 shows representative FTIR spectra for a monomer and the resulting polymer with the relevant peaks labeled along with an example area used to determine the conversion, and the conversion calculations for the C=C stretch at 1640 cm^{-1}. Percent conversion was calculated as one minus the ratio of the polymer peak area to the monomer peak area. FTIR was performed for sixteen monomer mixtures, consisting of all six base systems mentioned above, the six base systems +25 $_f$mol% BPAEDA(512) the three PETMP base systems +75 $_f$mol% BPAEDA(512), and pure BPAEDA(512). The thiol groups always appeared to convert fully, whereas the C=C stretch band and the allyl band indicated varying levels of conversion depending on the mixture composition.

Sol-fraction mass loss is shown in Fig. 10. 10TATATO mixtures lost the most mass, followed by 50TATATO mixtures. 90TATATO
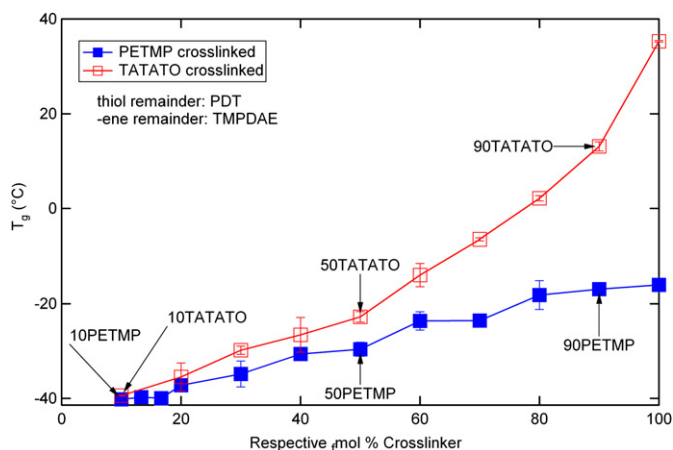
mixtures lost the least mass. In all three mixture bases, the addition of acrylate resulted in a larger mass loss. 10TATATO lost 11.3% of its initial mass while the addition of the acrylate caused the new mixture to lose 15.6%, a 38% increase in mass loss. 50TATATO lost 2.77% of its initial mass but 50TATATO + 25BPAEDA(512) lost 7.87%, a 184% increase. 90TATATO lost 0.80% of its initial mass while the same base mixture with added acrylate lost 3.81%, an increase of over 375%.

The final characterization technique used was mechanical testing of tensile strain-to-failure of the polymers. The compositions tested were the same ones shown in Figs. 7 and 8. Fig. 11 shows some representative stress–strain curves for the twenty-five selected mixtures. Failure by fracture is denoted by the 'x' in the figure. Figs. 12 and 13 show stress and strain at failure, respectively, for the twenty-five compositions. In general, the failure stress increases as the concentration of PETMP/TATATO and/or BPAEDA(512) increases in the mixture, while the failure strain decreases.

4. Discussion

As evident in Fig. 3, copolymers with high concentrations of PETMP behave as a typical thermoset network – a rubbery plateau region featuring a linear increase after reaching the "rubbery

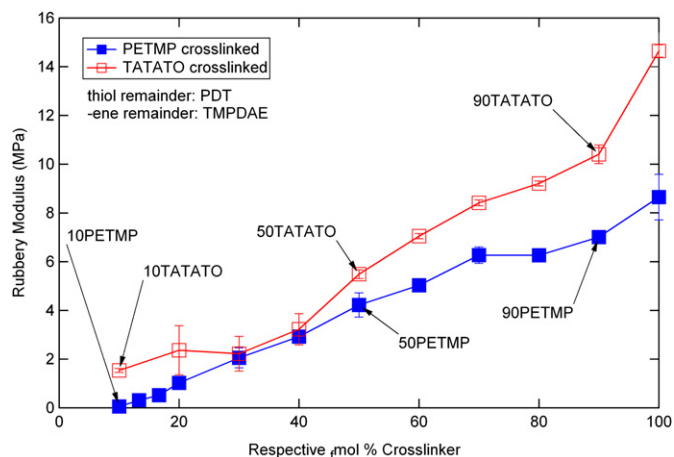Fig. 5. Glass transition temperatures for various ternary mixtures of TMPDAE and PDT with either PETMP or TATATO.
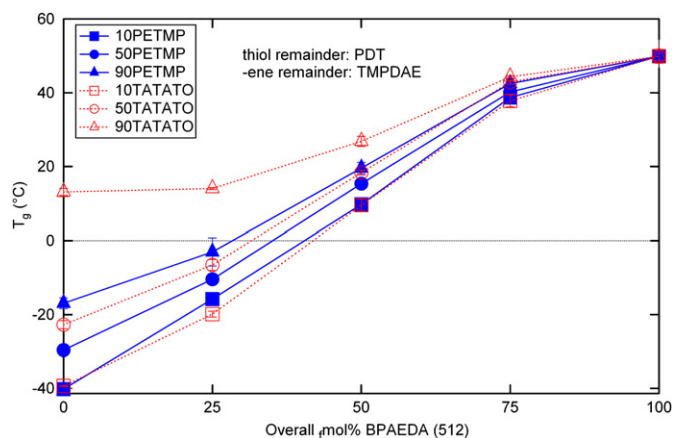

Fig. 7. Glass transition temperatures for (qua)ternary mixtures of thiol-ene/acrylate with various concentrations of acrylate added to the base thiol or –ene crosslinked system.
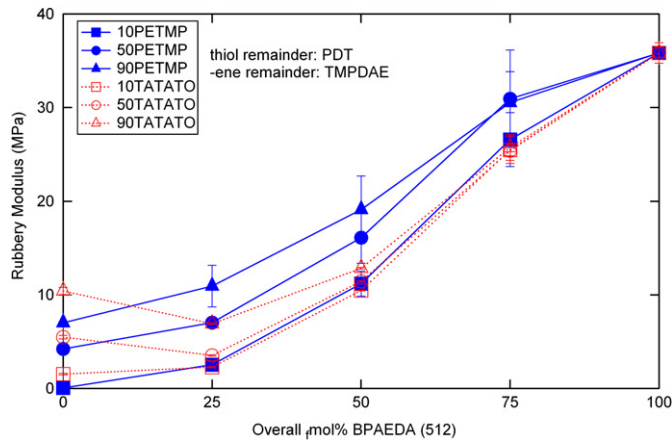
Fig. 8. Rubbery moduli for (qua)ternary mixtures of thiol-ene/acrylate with various concentrations of acrylate added to the base thiol or –ene crosslinked system.

modulus" minimum just after the transition. The material labeled 10PETMP behaves as a lightly-crosslinked elastomer at the very verge of the thermoset–thermoplastic limit, featuring a rubbery modulus two orders of magnitude lower than 100PETMP. Compositions featuring lower concentrations of PETMP did not yield

materials solid enough for handling, and so were excluded from the study; TATATO-crosslinked mixtures were made with matching crosslinker concentrations so that appropriate comparisons could be made and proper conclusions could be deduced. To determine if there was a PETMP concentration threshold for the switch from the elastomeric behavior of 10PETMP to the thermoset behavior of 20PETMP, two additional intermediate compositions, namely 13.33PETMP and 16.67PETMP, were synthesized and subjected to DMA testing. The results reveal that there is a smooth transition between the two behaviors.

There are two concurrent effects which contribute to the resulting T_g values of networks formed by various compositions of chemically different monomers, called the "copolymer effect" and the "crosslinking effect" [64–67]. The copolymer effect can raise or lower the T_g of a network, depending on the chemical rigidity of the monomers being added and subtracted, with more rigid structures corresponding to a higher T_g [65,66]. The crosslinking effect, on the other hand, serves solely to raise the T_g as additional chemical crosslink points hinder the mobility of the network. The separation of the two effects is not important for this study since it is the aggregate effect that concerns the networks' behavior, though the magnitudes of the contributions of the two effects for various copolymers have been determined in previous studies [65,68]. DMA testing reveals that both PETMP and TATATO have a crosslinking effect on the network, though TATATO appears to also
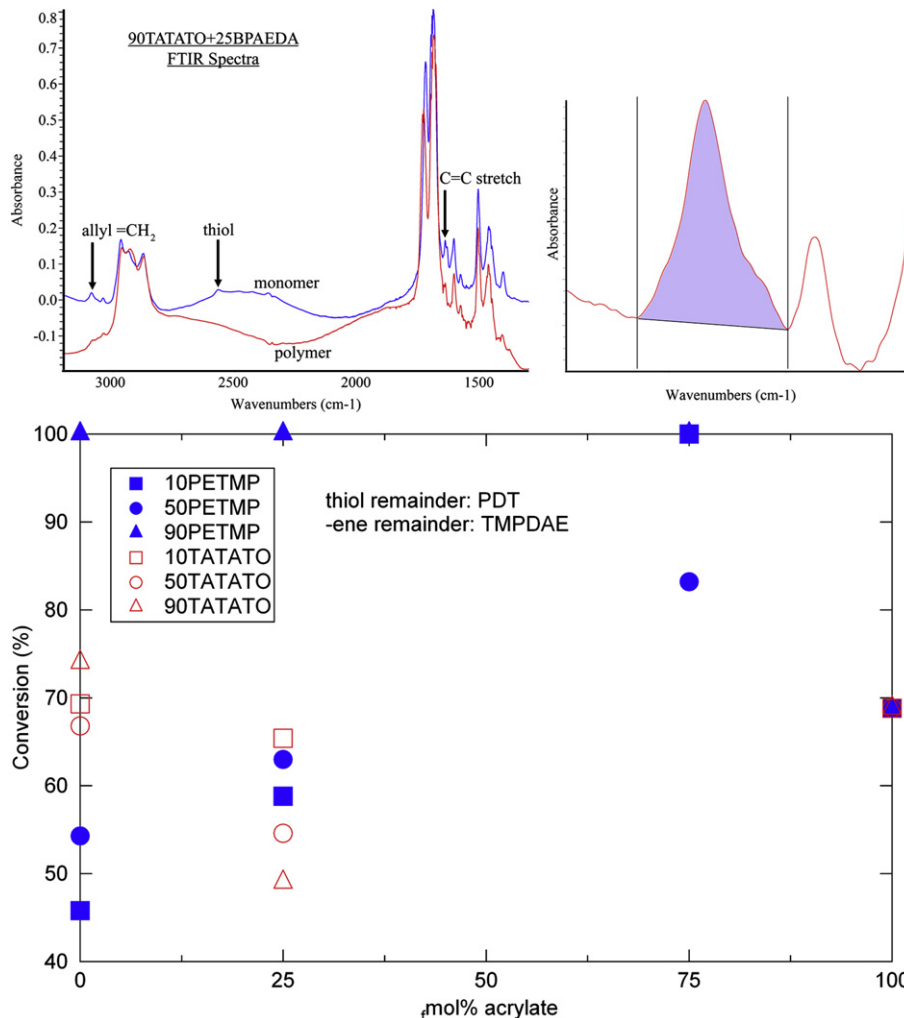

Fig. 9. (top left) Example FTIR spectra (top right) sample area used for peak calculation and (bottom) C=C conversion for various mixtures.
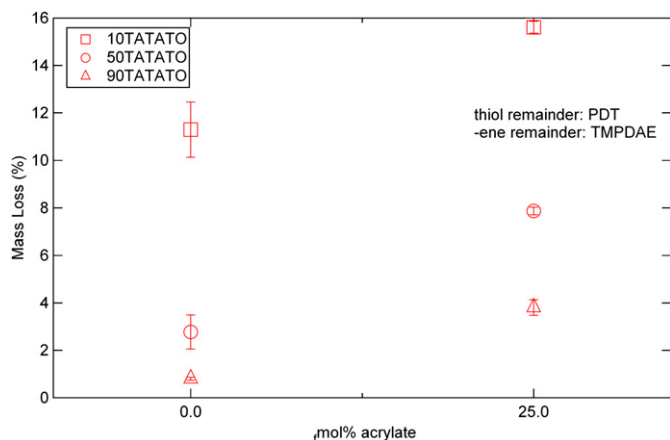
Fig. 10. Sol-fraction mass loss for six tested mixtures.

Fig. 12. Failure stress for (qua)ternary mixtures of thiol-ene/acrylate with various concentrations of acrylate added to the base thiol or –ene crosslinked system.

exhibit a T_g-raising copolymer effect, as will be discussed further in the following paragraph. The crosslinking effect can be observed in the increases in both the rubbery modulus and the glass transition temperature as the crosslinker concentration is increased (Figs. 3–6). Both of these increases can be attributed to an increased crosslink density, and, in the case of TATATO-containing mixtures, to monomer rigidity. Ideal rubber theory [69] states that the rubbery modulus is inversely proportional to the average molecular weight between crosslinks ($\overline{M}_c$), or directly proportional to the crosslink density, and this has been demonstrated to hold true for non-ideal (meth)acrylate networks as well [35].

As shown by Figs. 5 and 6, at the same concentration of crosslinking agent, TATATO-containing mixtures have a higher T_g and E_r than PETMP-containing mixtures. This can be expected given the structures of the crosslinkers – TATATO has a lower molecular weight per functional group and fewer functional groups per molecule than PETMP, and TATATO has a 6-membered ring core structure whereas PETMP consists of four longer, flexible "arms" connected at the center. The TATATO structure, therefore, will both increase T_g due to its core rigidity and raise rubbery modulus more than PETMP due to lower $\overline{M}_c$ at the same functional group concentration. Another contributing factor to TATATO mixtures' exhibition of higher T_g's and E_r's than those exhibited by PETMP mixtures (which is more evident at higher crosslinker concentrations as the properties diverge further) stems from the necessity for thiol and –ene functional group equivalence. As either crosslinker is
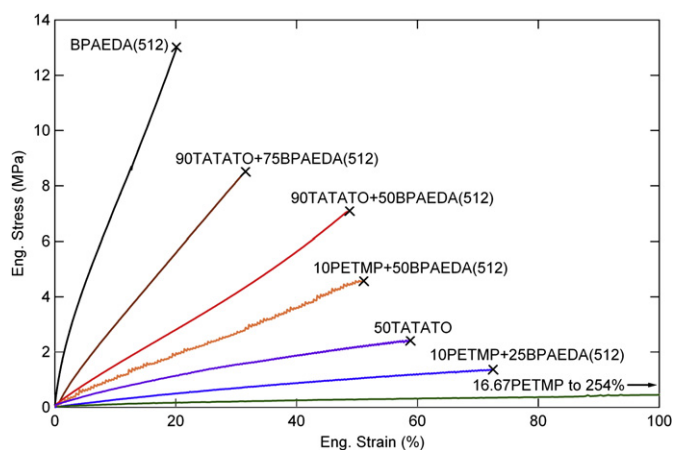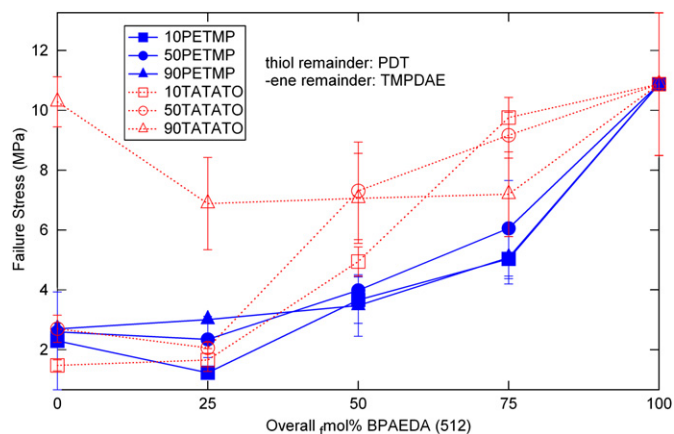

Fig. 11. Stress–strain behaviors for various thiol-ene/acrylate mixtures.

added, some difunctional monomer with the same functional group must be removed in proportion. Thus, as PETMP concentration increases in the mixtures, PDT concentration is reduced; as TATATO concentration increases, TMPDAE concentration decreases. PDT is replaced by a more flexible PETMP molecule, but this flexibility is counterbalanced by PETMP crosslinking and resulting network hindrances. TMPDAE, itself more flexible than PDT due to its larger number of unhindered bonds between functional groups, is replaced by an even stiffer cycle-cored TATATO – which has fewer bonds between functional groups in addition to acting as a crosslinker. Therefore, the trends, difference, and divergence of the properties of the two ternary mixture types shown in Figs. 5 and 6 can be explained when one considers that in PETMP mixtures the less flexible difunctional monomer is replaced by a more flexible crosslinker, while in TATATO mixtures the more flexible difunctional monomer is replaced by the least flexible monomer (which also acts as a crosslinker).

Except for 100TATATO, all of the ternary mixtures have T_g values which, being subambient, render such materials incapable of functioning in typical off-the-shelf shape memory applications. To remedy this situation[1] and increase the application space for these copolymers, a high-T_g monomer was added in the form of BPAEDA(512). However, the addition of BPAEDA(512) leads to a conflict in terms of E_r and T_g. A high T_g is desired so that the deformed state of the shape memory device is stable under ambient conditions, but a low E_r is desired since a low modulus generally translates to a larger deformation limit [35]. A low E_r would further increase the customizability of the network because the stress–strain behavior could be tuned by the introduction of different monomer chemistries. In the thiol-ene mixture, the acrylate can homopolymerize, adding a step to the reaction scheme shown in Fig. 1. BPAEDA(512) can act as an –ene and react with a thiol radical, thereby competing with TMPDAE and/or TATATO. Additionally, primary radicals from DMPA can initiate the BPAEDA(512) and create a carbon-centered acrylate radical. In either case, the carbon-centered acrylate radical can then abstract a hydrogen and propagate the thiol-ene reaction, or it can initiate more BPAEDA(512), forming a carbon-backbone acrylate chain.

---

[1] Efforts in this work to raise T_g using stiffer difunctional monomers, without excessive crosslinking (highly crosslinked shape memory polymers do not demonstrate adequate deformation levels), were unsuccessful and require further study.
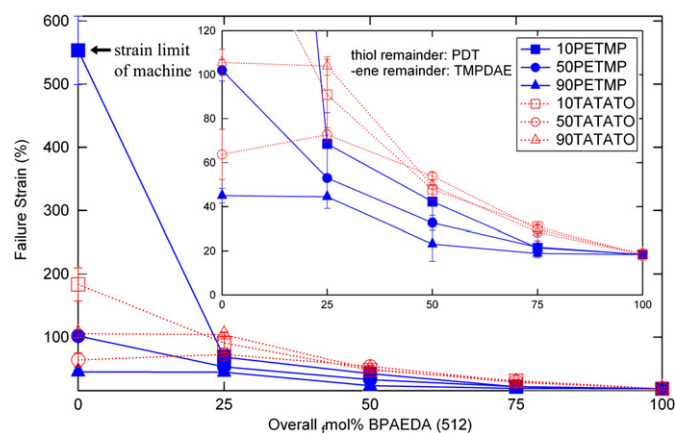
Fig. 13. Failure strain for (qua)ternary mixtures of thiol-ene/acrylate with various concentrations of acrylate added to the base thiol or –ene crosslinked system. Inset: low strain detail.

The incorporation of BPAEDA(512) via the thiol-ene reaction raises the T_g of the polymer by the copolymer effect since BPAEDA(512) simply acts as a linear chain "extender," while the homopolymerization route raises T_g and E_r by both the copolymer and the crosslinking effect. Figs. 7 and 8 show these anticipated effects when BPAEDA(512) is added. The drop in E_r in the TATATO + 25BPAEDA(512) quaternary mixtures compared to the acrylate-less ternary TATATO mixtures is most likely a plasticization effect caused by the larger amounts of dangling chain ends and residual monomer, which is confirmed by FTIR scans of the mixtures showing a lower conversion of –ene groups (Fig. 9). Larger reductions in E_r for these six mixtures correspond to greater drops in the overall C=C bond conversion. In the mixtures where TATATO is the crosslinker and BPAEDA(512) is added, the vinyl groups from the two monomers compete for reaction with the thiol groups, so some residual monomer is expected given the competitive reaction scheme. The effects of this competition are most prevalent in the TATATO + 25BPAEDA(512) mixtures because of the relatively low concentration of acrylate groups. Mixtures with higher concentrations of BPAEDA(512) have a significantly larger amount of pure acrylate network within the copolymer, simply because of the relative scarcity of thiol groups available for the typical thiol-ene reaction. These mixtures with larger acrylate networks certainly have some residual monomer and dangling chain ends, but these are percentagewise much smaller and so exert less of a negative effect on the resulting network properties than in the +25BPAEDA(512) copolymers.

Sol-fraction testing was used to determine the amount of soluble monomer that could be extracted from the networks based on the conversion data from FTIR. However, it was found that impurities dominated the response of the networks instead of overall conversion. As can be seen from a comparison of the pure base mixtures (0 $_f$mol% acrylate) in Fig. 10, mixtures with larger amounts of TMPDAE showed increased mass loss over those with larger amounts of the TATATO crosslinker. This increased mass loss is most likely the non-participating impurities associated with the TMPDAE monomer, which is only 90% pure as-received, while TATATO has a purity of 98%. However, the addition of acrylate to all of these systems increases the mass loss due to additional unconverted monomer being extracted, in agreement with the reduced conversion detected by FTIR. Large percentagewise increases in mass loss correlate well with large drops in conversion and large reductions in E_r. FTIR analysis cannot detect the presence of the non-participating impurities at the selected wavenumbers of

interest, so the reverse order of the mass loss magnitudes for +25 $_f$mol% acrylate compared to C=C conversion further supports the theory that impurities dominate the materials' sol-fraction behavior.

It is interesting to note that the mass loss from sol-fraction testing shows an inverse relationship with rubbery modulus, since higher mass losses are associated with lower rubbery moduli, or lower crosslink densities (and larger network openings). It is plausible that some unconverted bonds are termini for oligomers of various sizes, the larger of which cannot fit through the tighter networks. Alternatively, it is possible that many of the unconverted bonds detected by FTIR are on pendant, but attached chains which are not soluble but do not contribute to the network strength. However, without any further characterization of the eluent, it is difficult to conclude if the inverse relationship between mass loss and E_r truly exists or is merely an artifact of the increased impurity level associated with larger amounts of TMPDAE.

The stress–strain behavior of some sample mixtures is shown in Fig. 11, where failure by fracture is denoted by an x. The stress and strain at failure for the tested mixtures are summarized in Figs. 12 and 13. 10PETMP stretched the entire length of the thermal chamber and reached equipment limits before failure, further confirming its large strain behavior. The other base mixtures exhibited trends in strain and stress at failure which are consistent with results concerning (meth)acrylate networks [35], which found that higher concentrations of crosslinker reduce strain at failure but increase stress at failure. This behavior can be explained by considering the crosslink density, as implied by the DMA data discussed previously. Higher concentrations of crosslinker restrict the macromolecular motion of the network but increase the network's load-carrying capacity. Additionally, increased crosslink density generally means increased network heterogeneity [35,67,70], and with heterogeneity comes increased probability of a stress concentration arising due to a densely crosslinked area, which can cause a premature failure as compared to an ideally homogeneous network with the same overall crosslink density. The deviation of the 90TATATO and 90TATATO + 25BPAEDA(512) from the trends in stress and strain at failure can be attributed to the structure of TATATO. Both of these copolymers have rubbery moduli below about 10 MPa, which was determined by Safranski et al. [23] to be a threshold below which monomer chemistry plays a strong role in the (meth)acrylate network toughness and stress–strain behavior. They demonstrated that ringed members within a monomer allow the polymer to exhibit much higher toughness
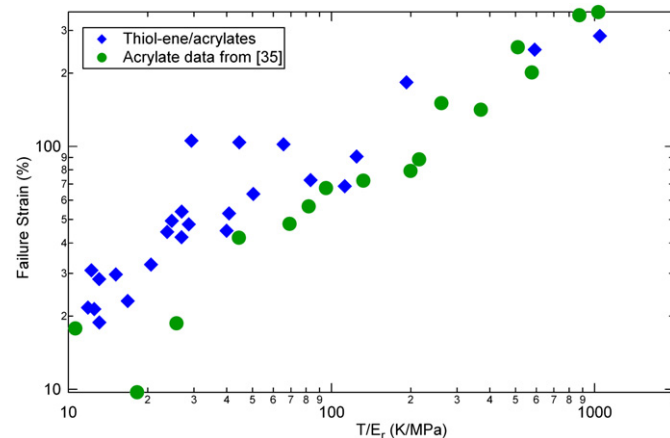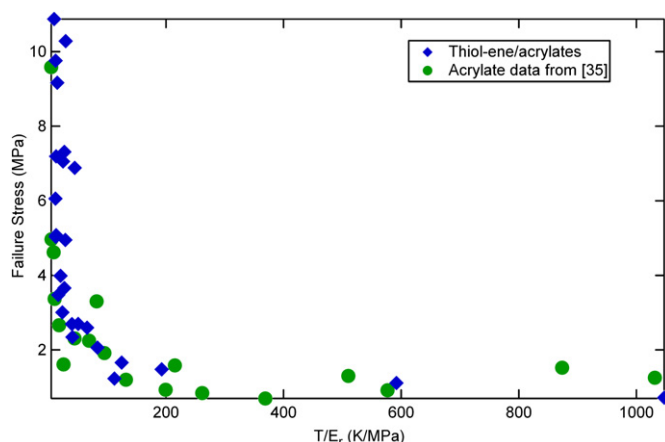

Fig. 14. Failure strain versus "molecular weight between crosslinks" following results of reference [35] for (qua)ternary mixtures of thiol-ene/acrylate with various concentrations of acrylate added to the base thiol or –ene crosslinked system.

Fig. 15. Failure stress versus "molecular weight between crosslinks" following results of reference [35] for (qua)ternary mixtures of thiol-ene/acrylate with various concentrations of acrylate added to the base thiol or –ene crosslinked system.

characteristics than polymers lacking rings; with the inclusion of a large amount of ring-cored crosslinker in 90TATATO and 90TATATO + 25BPAEDA(512), the enhanced strength and deformation characteristics can be expected.

Since strain and stress at failure are strongly related to the network structure and the density of crosslinking, it is instructive to graph these against the molecular weight between crosslinks $\overline{M}_c$, which is proportional to T/E_r. Figs. 14 and 15 show these data along with data from Ortega et al. [35], where T represents the temperature at which E_r is measured. The trend for strain vs. $\overline{M}_c$ is nearly linear, which agrees with previous results from peroxide-vulcanized rubbers by Morell and Stern in Treloar [69]. Additionally, these data also correspond quite well with the data from Ortega et al. [35] concerning (meth)acrylate networks, in which the data were also obtained by deforming the samples at a temperature at the peak of tan(δ). The data for stress vs. $\overline{M}_c$ also correspond very well with those from the (meth)acrylate study. This correspondence indicates that though there are important chemical implications as a result of the difference in the polymerization reactions, the overall mechanical effect of crosslinking a polymer results in similar system behaviors at T_g – highly crosslinked (low T/E_r) polymers have a higher stress at failure due to the increased load carrying capacity of the crosslink points while lightly
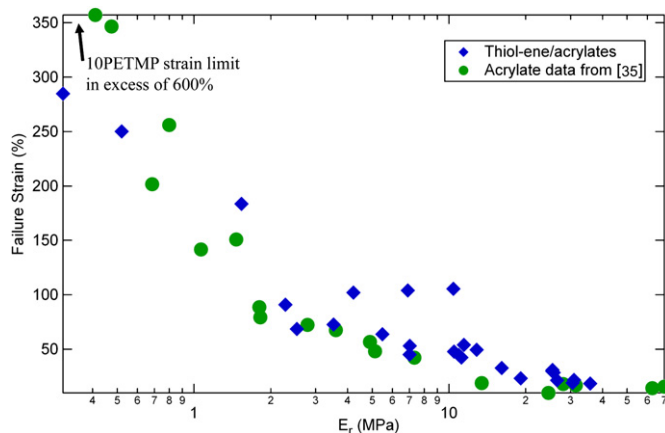
crosslinked materials (high T/E_r) have little strength but significant deformability.

Fig. 16, plotting strain at failure vs. E_r, highlights a major optimization tradeoff inherent to polymer design – the nonlinear and diminishing sensitivity of failure strain to rubbery modulus. Similar to the results from the (meth)acrylate study [35], strain at failure at low crosslink densities (or low E_r) is highly sensitive to rubbery modulus, but at higher modulus values the failure strain value changes much less. For example, an increase of the rubbery modulus from ~0.5 MPa to ~2.5 MPa results in a reduction of strain at failure from about 250% to about 100%, but an increase of the rubbery modulus from 10 MPa to 12 MPa results in minimal change in strain to failure.

5. Conclusions

Thiol-ene polymers are a versatile class that can incorporate acrylates to gain some of the benefits of acrylates while simultaneously avoiding some of the drawbacks of acrylates. The copolymer systems studied herein exhibited a broad range of tunable thermomechanical properties, such as T_g (−40 to 43 °C), E_r (<0.1 to 35 MPa), and failure strain (20% to >500%). Dynamic mechanical analysis revealed that the addition of thiol or –ene crosslinker increased T_g and E_r. Copolymers exploiting TATATO as a crosslinker exhibited higher T_g and E_r values than those with PETMP at the same concentration of crosslinker functional groups, due to the difference in the chemical structures.

The addition of BPAEDA(512) increased T_g and E_r due to both the copolymer and the crosslinking effect, except for three TATATO + 25 $_f$mol% BPAEDA(512) mixtures. These three mixtures exhibited lower E_r values due to dangling chains, the plasticization effect of residual monomer, and the competition of BPAEDA(512) and TATATO for thiyl radicals as confirmed by FTIR studies. FTIR spectroscopy shows that the addition of BPAEDA(512) to the mixture results in some unconverted –ene functional groups. The strict requirement for functional group equivalence in thiol-ene polymers is a limitation that can, to some degree, be alleviated by the addition of a homopolymerizing –ene such as an acrylate. Other authors have demonstrated how kinetic studies of the reaction can reveal the precise ratio of thiol:ene:acrylate needed to eliminate virtually all unreacted monomer. Sol-fraction testing elucidated the probable dominance of impurities on mass loss in solvent, but further testing is necessary for full characterization.

Higher crosslink densities, caused by large concentrations of BPAEDA(512) and/or PETMP/TATATO, generally result in higher stress and lower strain at failure as determined by tensile testing at T_g. These tensile results are in strong agreement with a previous study performed on (meth)acrylate systems. This work shows that various desired thermomechanical properties can be obtained by careful selection and mixing of various thiol-ene and acrylate monomers, but there are certain boundaries and tradeoffs that must always be taken into consideration.

The thermomechanical behavior of thiol-ene/acrylates and (meth)acrylate systems have excellent agreement at their respective T_g's and (meth)acrylate systems cover a broad range of achievable T_g values. Additionally, the mechanical properties of the two system types are quite similar at equivalent crosslink density. Therefore, future studies will investigate the other purported benefits of thiol-ene/acrylates as compared to (meth)acrylates to determine whether thiol-ene/acrylate systems occupy an application space that is outside the realm of (meth)acrylate systems' capabilities. Some of the application areas for these materials include small-scale biomedical devices and microfluidic mechanisms.

Fig. 16. Failure strain versus rubbery modulus following results of reference [35] for (qua)ternary mixtures of thiol-ene/acrylate with various concentrations of acrylate added to the base thiol or –ene crosslinked system.

Acknowledgements

References

[1] Wood JH. Frameless aircraft canopy actuation system and method. In: Office USP, ed. United States of Americaa, 2003.
[2] Spartech Corp., 2007.
[3] Krieg M, Weber C, and Szigeti P. Transparent plastic pane containing a copolymer of methylmethacrylate and polyfunctional acrylates. In: Office USP, ed. United States of America, 1997.
[4] Labra JJ. Journal of Aircraft 1982;19(6):480–4.
[5] Kent Periscopes Inc., 2008.
[6] Uniscope Optical Systems Inc., 2008.
[7] Yang S-J and Abel R. Stabilized UV transparent acrylic composition. In: Office USP, ed. United States of America, 2008.
[8] Hashida T, Ando E, and Goto Y. Optical storage media. In: Office USP, ed. United States of America, 1992.
[9] Ward JM. Plexiglas speakers. In: Office USP, ed. United States of America, 1976.
[10] Anan K, Murata Y, Amaya N, and Miyazaki T. Contact lens. In: Office USP, ed. United States of America, 1999.
[11] Plastics M. 2008.
[12] Santini AF. Washable acrylic paint. In: Office USP, ed. United States of America, 1994.
[13] Weiss P and Cheever GD. Powdered acrylic paint composition and method. In: Office USP, editor. United States of America, 1976.
[14] Junkin JH, Ginn ME, and Fronczak ET. Powder-resistant acrylic polymer floor finishes. In: Office USP, ed. United States of America, 1974.
[15] Everaerts AI, Purgett MD, and Momchilovich BS. Tackified acrylic adhesives. In: Office USP, ed. United States of America, 1994.
[16] Stow RH. Solvent-resistant pressure-sensitive adhesive tape. In: Office USP, ed., 1960.
[17] Edelman R and Catena WJ. Rapid curing structural acrylic adhesive. In: Office USP, ed. United States of America, 1999.
[18] Kondo K, Hoshida S, Aizawa M, and Amano T. Acrylic adhesive sheet. In: Office USP, ed. United States of America, 2008.
[19] Sawhney AS, Pathak CP, Hubbell JA. Macromolecules 1993;26(4):581–7.
[20] Sawhney AS, Pathak CP, Vanrensburg JJ, Dunn RC, Hubbell JA. Journal of Biomedical Materials Research 1994;28(7):831–8.
[21] West JL, Hubbell JA. Reactive Polymers 1995;25(2–3):139–47.
[22] Yakacki CM, Lyons MB, Rech B, Gall K, Shandas R. Biomedical Materials 2008;3(1).
[23] Safranski DL, Gall K. Polymer 2008.
[24] Anseth KS, Wang CM, Bowman CN. Polymer 1994;35(15):3243–50.
[25] Decker C. Surface Coatings International Part B-Coatings Transactions 2005;88(1):9–17.
[26] Decker C. Macromolecular Rapid Communications 2002;23(18):1067–93.
[27] Decker C. Polymer International 1998;45(2):133–41.
[28] Decker C, Bendaikha T, Decker D, Zahouily K. Abstracts of Papers of the American Chemical Society 1997;213. 210–POLY.
[29] Decker C, Elzaouk B, Decker D. Journal of Macromolecular Science-Pure and Applied Chemistry 1996;A33(2):173–90.
[30] Decker C. Acta Polymerica 1994;45(5):333–47.
[31] Decker C. Journal of Coatings Technology 1984;56(713):29–34.
[32] Anseth KS, Bowman CN. Abstracts of Papers of the American Chemical Society 1994;207:427.
[33] Dietz JE, Elliott BJ, Peppas NA. Macromolecules 1995;28(15):5163–6.
[34] Gall K, Yakacki CM, Liu YP, Shandas R, Willett N, Anseth KS. Journal of Biomedical Materials Research Part A 2005;73A(3):339–48.
[35] Ortega AM, Kasprzak SE, Yakacki CM, Diani J, Greenberg AR, Gall K. Journal of Applied Polymer Science 2008;110:1559–72.
[36] Yakacki CM, Shandas R, Lanning C, Rech B, Eckstein A, Gall K. Biomaterials 2007;28(14):2255–63.
[37] Posner T. Berichte der Deutschen Chemischen Gesellschaft 1905;38:646–57.
[38] Jacobine AF. Thiol-Ene photopolymers. In: Fouassier JP, Rabek JF, editors. Radiation curing in polymer science and technology. Polymerisation mechanisms, vol. III. New York: Elsevier Science Publishers, Ltd; 1993. p. 219–268.
[39] Jacobine AF, Glaser DM, Grabek PJ, Mancini D, Masterson M, Nakos ST, et al. Journal of Applied Polymer Science 1992;45(3):471–85.
[40] Kharasch MS, Nudenberg W, Mantell GJ. Journal of Organic Chemistry 1951;16(4):524–32.
[41] Szmant HH, Mata AJ, Namis AJ, Panthananickal AM. Tetrahedron 1976;32(22):2665–80.
[42] O'Brien AK, Cramer NB, Bowman CN. Journal of Polymer Science, Part a: Polymer Chemistry 2006;44(6):2007–14.
[43] Lu H, Carioscia JA, Stansbury JW, Bowman CN. Dental Materials 2005;21(12):1129–36.
[44] Carioscia JA, Lu H, Stanbury JW, Bowman CN. Dental Materials 2005;21(12):1137–43.
[45] Carioscia JA, Stansbury JW, Bowman CN. Polymer 2007;48(6):1526–32.
[46] Lee TY, Carioscia J, Smith Z, Bowman CN. Macromolecules 2007;40(5):1473–9.
[47] Kharasch MS, Read AT, Mayo FR. Chemistry and Industry 1938;57:752.
[48] Cramer NB, Bowman CN. Journal of Polymer Science, Part A: Polymer Chemistry 2001;39(19):3311–9.
[49] Senyurt AF, Wei HY, Hoyle CE, Piland SG, Gould TE. Macromolecules 2007;40(14):4901–9.
[50] Cramer NB, Davies T, O'Brien AK, Bowman CN. Macromolecules 2003;36(12):4631–6.
[51] Cramer NB, Reddy SK, O'Brien AK, Bowman CN. Macromolecules 2003;36(21):7964–9.
[52] Cramer NB, Scott JP, Bowman CN. Macromolecules 2002;35(14):5361–5.
[53] Lee TY, Smith Z, Reddy SK, Cramer NB, Bowman CN. Macromolecules 2007;40(5):1466–72.
[54] Reddy SK, Cramer NB, O'Brien AK, Cross T, Raj R, Bowman CN. Macromolecular Symposia 2004;206:361–74.
[55] Okay O, Bowman CN. Macromolecular Theory and Simulations 2005;14(4):267–77.
[56] Reddy SK, Cramer NB, Bowman CN. Macromolecules 2006;39(10):3673–80.
[57] Reddy SK, Cramer NB, Bowman CN. Macromolecules 2006;39(10):3681–7.
[58] Reddy SK, Okay O, Bowman CN. Macromolecules 2006;39(25):8832–43.
[59] Hoyle CE, Lee TY, Roper T. Journal of Polymer Science, Part A: Polymer Chemistry 2004;42(21):5301–38.
[60] Carioscia JA, Schneidewind L, O'Brien C, Ely R, Feeser C, Cramer N, et al. Journal of Polymer Science Part A-Polymer Chemistry 2007;45(23):5686–96.
[61] Rakas MA, Jacobine AF. Journal of Adhesion 1992;36(4):247–63.
[62] Senyurt AF, Wei H, Phillips B, Cole M, Nazarenko S, Hoyle CE, et al. Macromolecules 2006;39(19):6315–7.
[63] Gall K, Dunn ML, Liu Y, Finch D, Lake M, Munshi NA. Acta Materialia 2002;50:5115–26.
[64] Fox TG, Loshaek S. Journal of Polymer Science 1955;15(80):371–90.
[65] Loshaek S. Journal of Polymer Science 1955;15(80):391–404.
[66] Bicerano J, Sammler RL, Carriere CJ, Seitz JT. Journal of Polymer Science, Part B: Polymer Physics 1996;34(13):2247–59.
[67] Kannurpatti AR, Anseth JW, Bowman CN. Polymer 1998;39(12):2507–13.
[68] Greenberg AR, Kusy RP. Journal of Applied Polymer Science 1980;25(8):1785–8.
[69] Treloar LRG. The Physics of Rubber Elasticity. 2nd. ed. London: Oxford University Press; 1958.
[70] Young JS, Kannurpatti AR, Bowman CN. Macromolecular Chemistry and Physics 1998;199(6):1043–9.